

# Electrical current induced insulator-metal transition in tunnel junctions

J. V entura<sup>1,2</sup>, Z . Z hang<sup>3,4</sup>, Y . L iu<sup>3,5</sup>, J. B . S ousa<sup>1,2</sup> and P . P . F reitas<sup>1,3</sup>

<sup>1</sup> IN , Rua A lves Redol, 9-1, 1000-029 Lisbon, Portugal

<sup>2</sup> IF M UP , Rua do Cam po A legre, 678, 4169-007, Porto, Portugal

<sup>3</sup> IN E S C -M N , Rua A lves Redol, 9-1, 1000-029 Lisbon, Portugal

<sup>4</sup> D epartment of O ptical S cience and E ngineering, Fudan U niversity, Shanghai, China

<sup>5</sup> D epartment of P hysics, Tong ji U niversity, Shanghai, China

E-mail: joventur@fc.up.pt

PACS numbers: 73.40.R , 73.40.G k, 66.30.Q

**A bstract.** Current Induced Resistance S witching (CIS) was recently observed in thin tunnel junctions (TJs) with ferromagnetic (FM) electrodes and attributed to electromigration of metallic atoms in nanoconstrictions in the insulating barrier. The CIS effect is here studied in TJs with two thin (20Å) non-magnetic (NM) Ta electrodes inserted above and below the insulating barrier. We observe resistance (R) switching for positive applied electrical current (flowing from the bottom to the top lead), characterized by a continuous resistance decrease and associated with electromigration of metallic ions from the bottom electrode into the barrier (thin barrier state). For negative currents, displaced ions return into their initial positions in the electrode and the electrical resistance gradually increases (thick barrier state). We measured the temperature (T) dependence of the electrical resistance of both thin- and thick-barrier states ( $R_b$  and  $R_B$  respectively). Experiments showed a weaker R (T) variation when the tunnel junction is in the  $R_b$  state, associated with a smaller tunnel contribution. By applying large enough electrical currents we induced large irreversible R-decreases in the studied TJs, associated with barrier degradation. We then monitored the evolution of the R (T) dependence for different stages of barrier degradation. In particular, we observed a smooth transition from tunnel- to metallic-dominated transport. The initial degradation-stages are related to irreversible barrier thickness decreases (without the formation of pinholes). Only for later barrier degradation stages do we have the appearance of metallic paths between the two electrodes that, however, do not lead to metallic dominated transport for small enough pinhole radius.

## 1. Introduction

Tunnel junctions (TJ) are magnetic nanostructures consisting of two ferromagnetic (FM) layers separated by an insulator (I) [1]. The magnetization of one of the FM layers (pinned layer) is fixed by an underlying antiferromagnetic (AFM) layer. The magnetization of the other FM layer (free layer) reverses almost freely when a small magnetic field is applied. Due to spin dependent tunneling [2] one obtains two distinct resistance ( $R$ ) states corresponding to pinned and free layer magnetizations parallel (low  $R$ ) or antiparallel (high  $R$ ). Large tunnel magnetoresistive ratios of over 70% in  $\text{Al}_2\text{O}_3$  [3] and 150% in  $\text{MgO}$  [4, 5] (currently reaching more than 400% [6]) based tunnel junctions can be obtained, making them the most promising candidates for high performance, low cost, non-volatile magnetoresistive random access memories (MRAMs) [7]. Current research focus on replacing magnetic field-driven magnetization reversal by a Current Induced Magnetization Switching (CIMS) mechanism [8, 9]. Such goal was recently achieved in magnetic tunnel junctions [10, 11] for current densities  $j = 10^7 \text{ A/cm}^2$ . On the other hand, Liu et al. [12] observed reversible  $R$ -changes induced by lower current densities ( $j = 10^6 \text{ A/cm}^2$ ) in thin FM/I/FM TJs. These changes were found of non-magnetic origin [13] and attributed to electrical field-induced electromigration (EM) in nanoconstrictions in the insulating barrier [14, 15, 16]. This new effect, called Current Induced Switching (CIS) can limit the implementation of the CIMS mechanism in actual MRAMs, and its understanding is then crucial for device reliability.

The influence of Current Induced Switching on the behavior of the transport properties of AFM/FM/NM/I/NM/FM tunnel junctions is here studied in detail (NM non-magnetic). Resistance switching under relatively low positive electrical currents ( $I = 20 \text{ mA}$ ) produces a low resistance state due to local displacements (here, electromigration) of metallic ions from the bottom electrode into the barrier (thin barrier state). Applying sufficiently negative currents leads to the return of the displaced metallic ions from the barrier back into the electrode and so to an increase of the TJ-electrical resistance (thick barrier state), virtually displaying a reversible behavior. No time dependent phenomena were observed after each switching event [17], indicating that migrated Ta ions remain in deep energy minima inside the barrier. We compared the temperature ( $T$ ) dependence between 20 K and 300 K of the electrical resistance of the above junction thin- and thick-barrier states obtained after each switching ( $R_b$  and  $R_B$ , respectively), observing a smaller  $R(T)$  variation in the thin-barrier  $R_b$  state.

Applying large currents ( $|I|j & 80 \text{ mA}$ ) leads to irreversible resistance decreases due to enhanced barrier degradation. Successive switching under large  $|I|j$  produced a gradual evolution from tunnel- to metallic-dominated transport due to EM-induced barrier weakening. This effect initially starts with an irreversible mean barrier thickness decrease, followed by the establishment of metallic paths between the two electrodes. However, for small enough pinhole radius, tunnel still dominates transport ( $dR/dT < 0$ ) and only subsequent current-induced growth of pinhole size leads to a metallic-like temperature dependence ( $dR/dT > 0$ ).

## 2. Experimental details

We studied a series of ion beam deposited tunnel junctions, with thin non-magnetic Ta layers inserted just below and above the insulating  $\text{AlO}_x$  barrier. The corresponding complete structure was glass/bottom lead/Ta (90 Å)/NiFe (50 Å)/MnIr (90 Å)/CoFe (40 Å)/Ta (20 Å)/ $\text{AlO}_x$  (3 Å + 4 Å)/Ta (20 Å)/CoFe (30 Å)/NiFe (40 Å)/Ta (30 Å)/TiW (N) (150 Å)/top lead. Details on sample deposition and patterning processes were given previously [15]. Notice that the studied TJ-structure is similar to that of magnetic tunnel junctions grown for actual applications with the exception of the additional thin Ta layers, thus making comparisons with the FM/I/FM system easier. In particular, one can separate interface effects related to the particular metal layers bounding the oxide layer, from the spin polarization effects originated from the FM layers. Electrical resistance and current induced switching were measured with a standard four-point d.c. method. Temperature dependent measurements were performed (on cooling) in a closed cycle cryostat down to 20 K [18, 19]. CIS cycles were obtained using the pulsed current method [13], providing the remnant resistance value of the tunnel junction after each current pulse. We briefly describe some of the details used to measure CIS cycles [15]. Current pulses ( $I_p$ ) of 1 s duration are applied to the junction, starting with increasing pulses from  $I_p = 0$  (where we define the resistance as  $R_{\text{initial}}$ ) up to a maximum  $+I_{\text{max}}$ , in small  $I_p$  steps. The current pulses are then decreased through zero (half cycle,  $R = R_{\text{half}}$ ) down to negative  $-I_{\text{max}}$ , and then again to zero ( $R_{\text{nal}}$ ), to close the CIS hysteretic cycle. To discard non-linear I(V) contributions, the junction remnant resistance is measured between current pulses, always using a low current of 0.1 mA, providing a  $R(I_p)$  curve for each cycle. Positive current is here defined as flowing from the bottom to the top NM electrode. With the above definitions, one defines the CIS coefficient:

$$\text{CIS} = \frac{R_{\text{initial}} - R_{\text{half}}}{(R_{\text{initial}} + R_{\text{half}})/2}; \quad (1)$$

and the resistance shift ( $\Delta R$ ) in each cycle:

$$\Delta R = \frac{R_{\text{nal}} - R_{\text{initial}}}{(R_{\text{initial}} + R_{\text{nal}})/2}; \quad (2)$$

## 3. Experimental results

A FM/NM/I/NM/FM tunnel junction with  $R = 43$  and  $R_A = 170$  m (TJ1) was used to study Current Induced Switching. A CIS cycle spanning pulse currents up to  $I_{\text{max}} = 50$  mA is displayed in Fig. 1(b), giving CIS = 25% and  $\Delta R = 0.1\%$  at room temperature. With increasing (positive) applied current pulse, switching starts at  $I_p = 20$  mA through a progressive (but increasingly pronounced) R-decrease until  $I_{\text{max}} = 50$  mA. This switching is associated with local electromigration of Ta ions from the bottom electrode into the insulator [15], decreasing the effective barrier thickness and so the junction resistance (thin barrier state;  $R_b$ ). Even a small barrier weakening

considerably lowers the tunnel resistance due to its exponential dependence on barrier thickness. Furthermore, the switching is asymmetric with respect to the applied current direction, as observed in previous studies [16, 15] (only ions from the bottom interface participate in electromigration). This effect was related with the particular sequence of the deposition and oxidation processes during tunnel junction fabrication [16, 15].

Electromigration occurs when an applied electrical field biases the diffusive motion of atoms, so that a net atomic flux can be observed. The electromigration force is usually divided into two components, one in the direction of the electron flow (wind force) due to the transfer of momentum from electrons to the migrating ions. The other, acts in the direction of the electrical field (direct force) and is due to the electrostatic interaction between the electrical field and the direct valence of the ion [20]. Usually, the wind force is much larger than the direct force, making electromigration to occur in the direction of the electron flow. However, in our system, the ultra-thin barrier favors intense electrical fields thus enhancing field-directed diffusion (direct force dominance). Additionally, high applied electrical currents produce large heating and thus thermally enhanced electromigration [15]. Our results indicate that electromigration in our samples is essentially of a local character, ultimately causing pinhole formation (see below).

Returning to Fig. 1(b), the decrease of  $I_p$  from  $+I_{max}$  to zero hardly affects the low resistance state. This indicates that displaced Ta ions remain trapped in deep local energy minima inside the barrier. Such low  $R$ -state then persists for current pulses down to  $-35$  mA. However, when  $I_p < -35$  mA the (reversed sign) driving force gets strong enough to initiate the return of the displaced ions into their initial positions in the NM layer (causing an increase in  $R$ ), an effect which is rapidly enhanced until  $I_p = -I_{max}$ . We then have a thick barrier state ( $R_B$ ), i. e., completely recovering the previous (negative)  $R$ -switching which occurred near  $+I_{max}$ . The subsequent change of  $I_p$  from  $-I_{max}$  to zero, again leaves  $R$  essentially unchanged.

We then measured the temperature dependence of the electrical resistance of the TJ in its thick ( $R_B$ ) and thin ( $R_b$ ) barrier states [Fig. 1(a)]. The resistance of the  $R_B$  state steadily increases with decreasing  $T$  from  $R_B = 43$  at 300 K to 76 at  $T = 20$  K [Fig. 1(a)]. Defining the relative  $R$ -change between 300 K and 20 K as:

$$= \frac{R_{300K} - R_{20K}}{R_{300K}}; \quad (3)$$

so that  $\delta < 0$  ( $\delta > 0$ ) indicates tunnel (metallic) dominated transport, we obtain  $\delta_B = -78\%$  for the thick barrier state. On the other hand, after performing a positive half CITS cycle ( $0 \rightarrow I_{max} \rightarrow 0$ ) at room temperature [Fig. 1(b); open circles], the tunnel junction was left in its thin barrier state, following the  $R_b(T)$  measurements. The results now reveal a smaller  $R$ -increase from 300 K down to 20 K ( $R_b = 32$  and 53, respectively) than in the  $R_B(T)$  case, giving  $\delta_b = -66\%$ , and so  $\delta_B < \delta_b < 0$ .

The  $R_B(T)$  and  $R_b(T)$  curves were fitted to the expressions for two- and three-step hopping [21] and phonon-assisted tunneling [22], revealing a decrease of the hopping contributions and a slight increase of the phonon-assisted tunneling when one goes from  $R_B$  to the  $R_b$  state. This is here attributed to the decrease of the barrier thickness

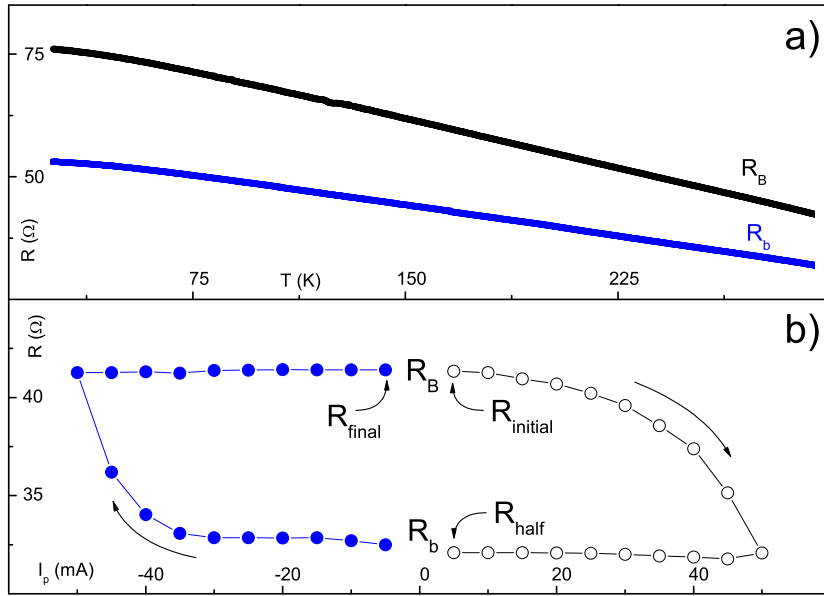


Figure 1. (a) Temperature dependence of the electrical resistance in the low ( $R_b$ ; thin barrier) and high ( $R_B$ ; thick barrier) C IS states of TJ1. (b) Half C IS cycle performed with  $I_{\text{max}} = 50$  mA (open circles) that enabled us to change from the (initial) thick to the thin barrier state; subsequent half C IS cycle recovering the thick barrier state (full circles) and displaying a reversible behavior.

(reducing the hopping contribution) and to enhanced excitation of phonons at the electrodes/oxide interface, by tunneling electrons.

We also studied the effect of increasing barrier degradation on the (subsequent) temperature dependence of the electrical resistance of a tunnel junction. For this we performed C IS cycles with high  $I_{\text{max}}$  (in the 80{110 mA range), each successive one showing a large negative shift at room temperature ( $R_{\text{nal}} - R_{\text{initial}}$ ), indicating a progressive and irreversibly barrier weakening [15]. After each  $n$ -th room temperature C IS cycle, we always measured  $R(T)$  from 300 to 20 K. No temperature hysteresis was observed, so that on heating back to room temperature, the  $n$ -th value of the TJ-resistance is essentially recovered. On the other hand, with increasing ( $n$ ) cycling, the junction transport changed smoothly from tunnel- ( $dR/dT < 0$ ) to metallic-dominated [ $dR/dT > 0$ ; Fig. 2(a)]. Two tunnel junctions were used in this particular study: TJ2 with initial  $R = 11.3$  ( $R/A = 67.8$  m $^2$ ) and TJ3 with  $R = 21.6$  ( $R/A = 259.2$  m $^2$ ).

Both TJs initially ( $n = 0$ ; before any C IS cycle) exhibit a tunnel-dominated  $R(T)$  behavior with  $= 20\%$  and  $75\%$ , for samples TJ2 and TJ3 respectively (notice the smaller  $R/A$  product of TJ2). Subsequent C IS cycles with large  $I_{\text{max}}$  led to irreversible decreases of the TJs resistance and to a steady increase of in both samples [Fig. 2(a)]. Nevertheless, our  $R(T)$  data still showed tunnel-dominated transport ( $< 0$ ) down to  $R/A = 20$  m $^2$ . The last  $R(T)$  measurement with tunnel-dominated behavior displayed  $= 3\%$  for TJ2 ( $n = 6$ ;  $R = 2.5$ ) and  $= 15\%$  for

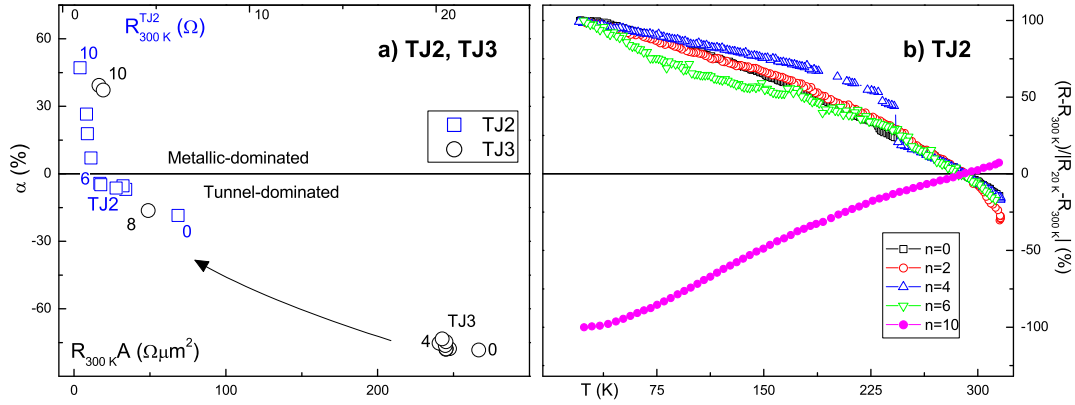


Figure 2. (a) The relative resistance change from 300 K to 20 K ( ) as a function of the  $R \cdot A$  product (lower scale; for TJ2 and TJ3) and  $R_{300K}$  (upper scale; TJ3 only). Resistance decrease was induced by EM -driven barrier degradation under high applied current pulses. The numbers in the Figure indicate how many CIS cycles were performed before the corresponding -data point was obtained. (b) Selected normalized  $R(T)$  curves in the 300{20 K range (TJ2).

TJ3 ( $n = 8$ ;  $R = 5$  ). Finally, further cycling ultimately leads to metallic behavior, with e. g.  $\alpha = 47\%$  for TJ2 ( $n = 10$ ;  $R = 0.65$  ) and  $\alpha = 40\%$  for TJ3 ( $n = 10$ ;  $R = 1.9$  ), evidencing the formation of pinholes in the barrier.

We then normalized our  $R(T)$  data according to  $\frac{R(T)}{R_{20K}} \frac{R_{300K}}{R_{300K}}$ . Figure 2 (b) displays selected curves for different stages of barrier degradation (sample TJ2), obtained after performing the corresponding  $n$ -th CIS cycle. Although the shapes of the (tunnel dominated) curves are almost equal, some display increasing  $R$ -steps. On the other hand, the normalized metallic-dominated transport curves ( $n > 6$ ) are all identical.

#### 4. Discussion

We showed that local electromigration effects cause irreversible resistance decreases and a progressive change of the dominant transport mechanism from tunnel to metallic, due to the interplay of two main contributions: Tunnel through the undamaged part of the barrier (with resistance  $R_t$ ) and metallic transport through pinholes (resistance  $R_m$ ). We then write for the measured resistance ( $R$ ):

$$\frac{1}{R} = \frac{1}{R_t} + \frac{1}{R_m} : \quad (4)$$

We can estimate the evolution of pinhole size with decreasing TJ-resistance due to barrier degradation. The Sharvin theory predicts the resistance of a nanoconstriction modeled as a circular aperture of radius  $a$  (between two metallic layers) of electrical resistivity  $\rho$  and electron mean free path  $\lambda$  [23]. We then have in the ballistic limit ( $\lambda > > a$ ):

$$R_m (\text{Sharvin}) = \frac{4 \cdot \rho}{3 \cdot a^2} : \quad (5)$$

Since the amorphous Ta layers of the studied TJs have a high resistivity ( $\sim 150 \text{ }\Omega\text{-cm}$ ) [15], we do not expect the electron mean free path ' within a pinhole to be very large ('. a). We thus write the electrical resistance of a constriction in the dissipative regime ('  $\ll a$ ), known as the Maxwell resistance [24]:

$$R_m (\text{Maxwell}) = \frac{\pi}{2a} : \quad (6)$$

A good approximation for the actual pinhole resistance ( $R_m$ ) of a sample with ' is simply [24, 25, 26]:

$$R_m = R_m (\text{Maxwell}) + R_m (\text{Sharvin}) : \quad (7)$$

To calculate the pinhole radius, let us assume that i) a pinhole is formed just after an irreversible resistance decrease under high applied current pulses; ii) only one pinhole is formed and grows in the tunnel junction and, iii) the tunnel resistance remains constant throughout the successive CIS degrading stages (significant R-variation only arises from the enhancement of the metallic contribution). Accordingly,  $R_t$  is simply the tunnel junction resistance measured before EM-induced barrier degradation ( $R_t = 11$  for TJ2 and  $R_t = 22$  for TJ3). This allows us to estimate the metallic resistance  $R_m$  using Eq. (4) and the measured R-value [see Fig. 3(b)]. Using Eqs. (5)–(7), we can then express the pinhole radius as a function of ' and  $R_m$ :

$$a = \frac{3 + \frac{p}{3} \frac{p}{64 R_m + 3}}{12 R_m} : \quad (8)$$

Using  $\sim 150 \text{ }\Omega\text{-cm}$  for the Ta layers (and pinholes) and assuming ' = 5A, we can then estimate the pinhole radius [Fig. 3(a)]. Notice that the actual pinhole composition is not entirely known, and the possibility of Ta-Al bonding cannot be excluded. However, the migration of the Ta ions into the amorphous Al<sub>2</sub>O<sub>3</sub> barrier should give rise to a disordered pinhole structure with a high resistivity. For TJ3, as expected, one obtains a pinhole radius which increases with decreasing resistance: from about 30 A for  $n = 4$  ( $R_m = 250$ ) to 1500 A for  $n = 8$  ( $R_m = 5$ ), and finally to 4300 A for  $n = 10$  ( $R_m = 1.7$ ). Notice however that this simple model does not fully describe our data. In particular, it underestimates the metallic resistance: For  $n = 8$  (for which we still observe tunnel dominated transport;  $\beta < 0$ ) we obtain  $R_m = 5$ , which is already smaller than the (assumed constant) tunnel resistance,  $R_t = 22$ . Our model then predicts a metallic R(T) behavior for  $n = 8$ , which contradicts our data. Notice that such  $R_m$  value depends only on  $R_t$  used in Eq. (4) and not on ' or ' which are used only to estimate a.

We conclude that the initial EM-driven irreversible resistance decrease is not due to the formation of pinholes [assumption (i)] but to the progressive weakening of the tunnel barrier (decreasing barrier thickness) and that the minimum experimental R-value without pinholes ( $R = R_t$ ) is considerably lower than the initial TJ resistance of 22. Using Eq. (4), we estimate that, to ensure  $R_t > R_m$  up to  $n = 8$  we must have  $R_t = 8$ . Then, the initial 22 ! 8 R-decrease corresponds only to a barrier thickness reduction (t) without the formation of pinholes. We estimate t = 1.3A [15].

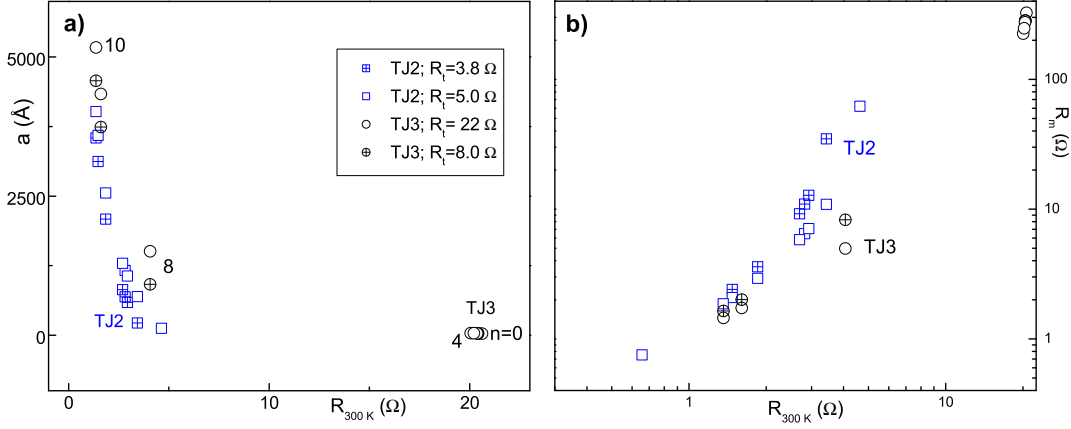


Figure 3. (a) Pinhole radius  $a$ , calculate using Eq. (8), as a function of the experimental tunnel junction electrical resistance [TJ2 using  $R_t = 3.8$  (open squares) and  $R_t = 5$  (squares with crosses) and TJ3 using  $R_t = 22$  (open circles) and  $R_t = 8$  (circles with crosses); see discussion for details]. (b) Corresponding metallic resistance  $R_m$ , as calculated from Eq. (4).

Assuming then  $R_t = 8$ , we can calculate the new pinhole radius using Eq. (8) [Fig. 3(a)]. For  $n = 10$  we obtain  $a = 900\text{ }\text{\AA}$  ( $R_m = 8.3$ ) and for  $n = 12$ ,  $a = 3700\text{ }\text{\AA}$  ( $R_m = 2.0$ ), which, nevertheless, are close to the values obtained above (considering  $R_t = 22$ ). Furthermore,  $R_t = 8$  is not the only value that adequately adapts to the observed ( $R$ ) dependence and we estimate  $3.5 \leq R_t \leq 8$ . For  $R_t = 3.5$  one has pinhole formation only for  $n = 11$ , already having  $R_m < R_t$  ( $a = 2500\text{ }\text{\AA}$ ). In this case ( $R_t = 3.5$ ), the formation of a pinhole immediately leads to metallic-dominated transport.

For TJ2, we have more  $n$ -values near the tunnel/metallic progressive transition, allowing us to estimate  $R_t$  within a narrower interval. First, notice that (as in the case of TJ3) if we use the initial TJ2-resistance ( $R_t = R = 11\text{ }\Omega$ ) to calculate  $R_m$ , we again obtain  $R_m < R_t$  for a  $R(T)$  data still dominated by tunneling ( $n < 0$ ). Thus, we again conclude on the initial progressive weakening of the tunnel barrier (decreasing barrier thickness), leading to the decrease of the TJ electrical resistance without formation of pinholes. We predict [using Eq. (4)] that  $3.8 \leq R_t \leq 5$  [Fig. 3], which corresponds to a barrier thickness decrease satisfying  $1.1\text{ }\text{\AA} \leq a \leq 1.3\text{ }\text{\AA}$ . Using the two mentioned limiting  $R_t$ -values, we again observe that  $R_m$  decreases with decreasing TJ electrical resistance [Fig. 3(b)], denoting the increase of pinhole radius [Fig. 3(a)]. In the case of TJ2, we observe that pinholes are already formed ( $a = 1000\text{ }\text{\AA}$ ) while  $n < 0$  (demonstrating tunnel dominated transport;  $R_m > R_t$ ). Further current-induced decrease of the TJ resistance is seen to be due to the growth of the pinhole size, which enhances the metallic conductance and ultimately leads to metallic-dominated transport ( $n > 0$ ).

## 5. Conclusions

We showed that the initial insulating barrier degradation under high electrical currents arises from irreversible barrier thickness decrease ( $t = 1.3\text{ \AA}$ ) due to localized electromigration of ions from the electrodes into the barrier, without the formation of pinholes. Such barrier weakening leads to higher values in our  $R_b(T)$  and  $R_B(T)$  measurements (with  $b > B$ ), suggesting that irreversible and reversible switching arise from the same physical mechanism. Under adequate experimental conditions we might even reversibly switch between  $B < 0$  (tunnel-dominated transport) and  $b > 0$  (metallic-dominated transport), and vice-versa, by local electromigration. Such phenomenon was recently observed by Deac et al. [14] in ultra-thin TJs (barrier thickness  $t = 5\text{ \AA}$ ).

Increased barrier degradation leads to the formation of metallic paths between the two electrodes that, however, do not lead to a metallic-dominated TJ transport for small enough pinhole radius. The increase of such radius gradually leads to the decrease of the metallic (Shawin+ Maxwell) resistance and thus to the ultimate dominance of metallic over tunnel transport.

## Acknowledgments

Work supported in part by FEDER-POCTI/0155, POCTI/CTM/45252/02 and POCTI/CTM/59318/2004 from FCT and IST-2001-37334 NEXT MRAM projects. J. Ventura is thankful for a FCT post-doctoral grant (SFRH/BPD/21634/2005).

## References

- [1] J. S. Moodera, L. R. Kinder, T. M. Wong, and R. Meservey. Large magnetoresistance at room temperature in ferromagnetic thin film tunnel junctions. *Phys. Rev. Lett.*, 74:3273{3276, April 1995.
- [2] R. Meservey and P. M. Tedrow. Spin-polarized electron tunneling. *Phys. Rep.*, 238:173{243, March 1994.
- [3] D. Wang, C. Nordman, J. M. Daughton, Q. Zhenghong, and J. Fink. 70% TMR at room temperature for SDT sandwich junctions with CoFeB as free and reference layers. *IEEE Trans. Magn.*, 40:2269{2271, July 2004.
- [4] S. S. P. Parkin, C. Kaiser, A. Panchula, P. M. Rice, B. Hughes, M. Samant, and S. H. Yang. Giant tunnelling magnetoresistance at room temperature with MgO (100) tunnel barriers. *Nature Mat.*, 3:862{867, December 2004.
- [5] S. Yuasa, T. Nagahama, A. Fukushima, Y. Suzuki, and K. Ando. Giant room-temperature magnetoresistance in single-crystal Fe/MgO/Fe magnetic tunnel junctions. *Nature Mat.*, 3:868{871, December 2004.
- [6] S. Yuasa, A. Fukushima, H. Kubota, Y. Suzuki, and K. Ando. Giant tunneling magnetoresistance up to 410% at room temperature in fully epitaxial Co/MgO/Co magnetic tunnel junctions with bcc Co(001) electrodes. *Appl. Phys. Lett.*, 89:042505, July 2006.
- [7] S. Tehrani, B. Engel, J. M. Slaughter, E. Chen, M. de Herrera, M. Durlam, P. Naj, R. Whig, J. Janesky, and J. Calder. Recent developments in magnetic tunnel junction MRAM. *IEEE Trans. Magn.*, 36:2752{2757, September 2000.

[8] J. C. Słonczewski. Current-driven excitation of magnetic multilayers. *J. Magn. Magn. Mater.*, 159:L1{L7, June 1996.

[9] L. Berger. Emission of spin waves by a magnetic multilayer traversed by a current. *Phys. Rev. B*, 54:9353{9358, October 1996.

[10] Y. Huai, F. A. Ibert, P. N. Guyen, M. Pakala, and T. Valet. Observation of spin-transfer switching in deep submicron-sized and low-resistance magnetic tunnel junctions. *Appl. Phys. Lett.*, 84:3118{3120, April 2004.

[11] G. D. Fuchs, N. C. Emley, I. N. Kriegerov, P. M. Braganca, E. M. Ryan, S. I. Kiselev, J. C. Sankey, D. C. Ralph, R. A. Buhrman, and J. A. Katine. Spin-transfer effects in nanoscale magnetic tunnel junctions. *Appl. Phys. Lett.*, 85:1205{1207, August 2004.

[12] Y. Liu, Z. Zhang, P. P. Freitas, and J. L. Martins. Current-induced magnetization switching in magnetic tunnel junctions. *Appl. Phys. Lett.*, 82:2871{2873, April 2003.

[13] Y. Liu, Z. Zhang, and P. P. Freitas. Hot-spot mediated current-induced resistance change in magnetic tunnel junctions. *IEEE Trans. Magn.*, 39:2833{2835, September 2003.

[14] A. Deac, O. Redon, R. C. Sousa, B. Djeny, J. P. Nozieres, Z. Zhang, Y. Liu, and P. P. Freitas. Current driven resistance changes in low resistance  $x$  area magnetic tunnel junctions with ultra-thin  $\text{AlO}_x$  barriers. *J. Appl. Phys.*, 95:6792{6794, June 2004.

[15] J. Ventura, J. B. Sousa, Y. Liu, Z. Zhang, and P. P. Freitas. Electromigration in thin tunnel junctions with ferromagnetic/nonmagnetic electrodes: Nanoconstrictions, local heating, and direct and wind forces. *Phys. Rev. B*, 72:094432, September 2005.

[16] J. Ventura, J. Araújo, J. B. Sousa, Y. Liu, Z. Zhang, and P. P. Freitas. Nanoscopic processes of Current Induced Switching in thin tunnel junctions. *IEEE Trans. Nanotechnol.*, 5:142{148, March 2006.

[17] J. Ventura, J. Araújo, F. Carpinho, J. B. Sousa, Y. Liu, Z. Zhang, and P. P. Freitas. Relaxation Phenomena in Current Induced Switching in Thin Magnetic Tunnel Junctions. *J. Magn. Magn. Mater.*, 290:1067{1070, April 2005.

[18] J. O. Ventura, J. B. Sousa, M. A. Salgueiro da Silva, P. P. Freitas, and A. Veloso. Nonlocal magnetoresistance behavior of CoFe nano-oxide spin valves at low temperatures. *J. Appl. Phys.*, 93:7690{7692, May 2003.

[19] J. Ventura, J. P. Araújo, J. B. Sousa, R. Ferreira, and P. P. Freitas. Competing spin-dependent conductance channels in under-oxidized tunnel junctions. *Appl. Phys. Lett.*, 90:032501, Jan 2007.

[20] R. S. Sorbello. Theory of electromigration. In H. Ehrenreich and F. Spaepen, editors, *Solid State Physics*, volume 51, pages 159{231. Springer-Verlag, New York, 1998.

[21] C. H. Shang, J. Nowak, R. Jansen, and J. S. Moodera. Temperature dependence of magnetoresistance and surface magnetization in ferromagnetic tunnel junctions. *Phys. Rev. B*, 58:R2917{R2920, August 1998.

[22] T. D. Imopoulou, G. G. Jéres, J. W. Ecker, Y. Luo, and K. Samwer. Analysis of the magnetotransport channels in tunnel junctions with amorphous CoFeB. *Europhys. Lett.*, 68:707{712, December 2004.

[23] Yu. V. Sharvin. A possible method for studying Fermi surfaces. *J. Exptl. Theoret. Phys.*, 48:984{985, March 1965.

[24] G. Wexler. The size effect and the non-local Boltzmann transport equation in orifice and disk geometry. *Proc. Phys. Soc.*, 89:927{941, June 1966.

[25] K. S. Ralls and R. A. Buhrman. Microscopic study of noise in metalnanobridges. *Phys. Rev. B*, 44:5800{5817, September 1991.

[26] B. Nikolic and P. B. Allen. Electron transport through a circular constriction. *Phys. Rev. B*, 60:3963{3969, August 1999.